Probing gluon saturation and nuclear structure in photon-nucleus collisions

Heikki Mäntysaari
with F. Salazar, B. Schenke, C. Shen, W. Zhao
arXiv:2312.04194 & arXiv:2310.15300 & in preparation

University of Jyväskylä
Centre of Excellence in Quark Matter
Finland

DIS2024, April 10, 2024

Introduction: vector mesons in UPCs, $A+A \to J/\psi + A + A$

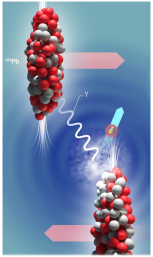

D. Grund, UPC2023

Two-fold ambiguity:

$$x_A = \frac{M_V}{\sqrt{s}} e^{\pm y}$$

$$\sigma \sim n_\gamma(+y)\sigma(+y) + n_\gamma(-y)\sigma(-y)$$

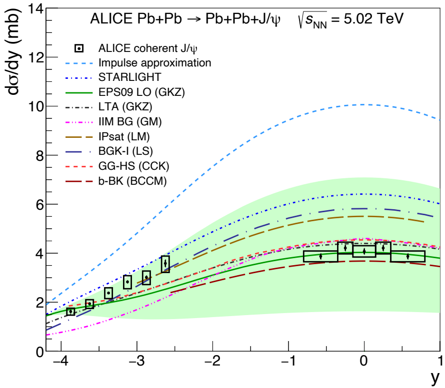

In principle UPCs provide access to very small-x nuclear structure, but high-x_A component dominates at large $|y|$

ALICE, 2101.04577

Recent development: extract individual $\gamma + A$ contributions

$$\frac{\mathrm{d}\sigma_{AA}^{\{b_1\}}}{\mathrm{d}y} = n_\gamma(y, \{b\}_1)\sigma_{\gamma A}(y) + n_\gamma(-y, \{b\}_1)\sigma_{\gamma A}(-y)$$

$$\frac{\mathrm{d}\sigma_{AA}^{\{b_2\}}}{\mathrm{d}y} = n_\gamma(y, \{b\}_2)\sigma_{\gamma A}(y) + n_\gamma(-y, \{b\}_2)\sigma_{\gamma A}(-y)$$

Forward neutron classes $\Rightarrow$ impact parmeter range $\{b_i\}$ $\Rightarrow$ different flux n_γ

$\Rightarrow$ solve for $\sigma_{\gamma A}$ Method: Guzey et al, 1312.6486

See talk by Contreras (Tue) for details

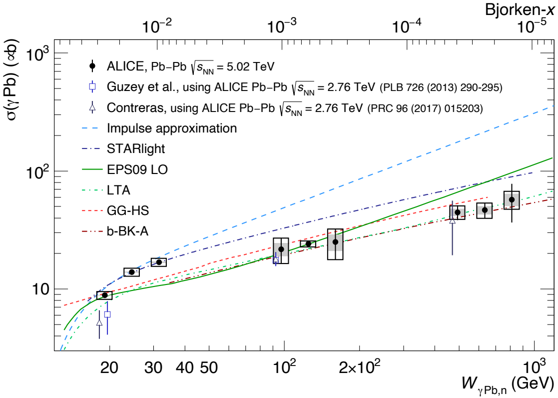

Access VM production at very small x

Confront CGC calculations with this data!

ALICE, 2305.19060

Coherent and incoherent vector meson production

Coherent

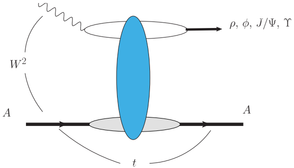

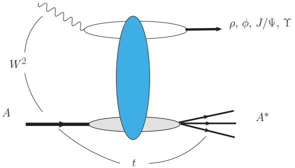

Incoherent

Figure: 2007.13625

Coherent: target remains intact, initial state $|i\rangle$ = final state $|f\rangle$.

Good, Walker, Phys. Rev. 1960:

$$\frac{\mathrm{d}\sigma^{\text{coherent}}}{\mathrm{d}t} \sim |\langle\mathcal{A}\rangle_\Omega|^2$$

$\Rightarrow$ Probe average interaction $\Rightarrow$ average geometry

Coherent and incoherent vector meson production

Coherent

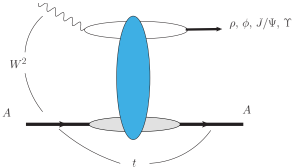

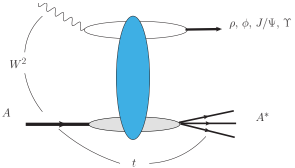

Incoherent

Figure: 2007.13625

Coherent: target remains intact, initial state $|i\rangle$ = final state $|f\rangle$.

Good, Walker, Phys. Rev. 1960:

$$\frac{\mathrm{d}\sigma^{\text{coherent}}}{\mathrm{d}t} \sim |\langle \mathcal{A} \rangle_\Omega|^2$$

$\Rightarrow$ Probe average interaction $\Rightarrow$ average geometry

Incoherent: $|i\rangle \neq |f\rangle$: target breaks up:

$$\frac{\mathrm{d}\sigma^{\text{incoh}}}{\mathrm{d}t} = \frac{\mathrm{d}\sigma^{\text{total diff}}}{\mathrm{d}t} - \frac{\mathrm{d}\sigma^{\text{coherent}}}{\mathrm{d}t} \sim \left\langle |\mathcal{A}|^2 \right\rangle_\Omega - \left| \left\langle \mathcal{A} \right\rangle_\Omega \right|^2$$

Variance $\Rightarrow$ access to event-by-event fluctuations in the target structure

Vector meson production at high energy

$$\gamma + A \to (\mathrm{J}/\psi, \rho, \dots) + A$$

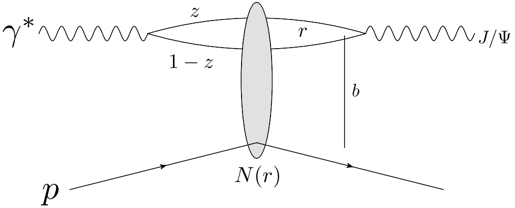

Lowest order in perturbation theory:

$$\mathcal{A}_\Omega \sim i \int \mathrm{d}^2\mathbf{b}_\perp\, e^{-i\mathbf{b}_\perp\cdot\mathbf{\Delta}} \Psi^* \otimes \Psi_{\mathrm{J}/\psi} \otimes N_\Omega$$

1. $\gamma^* \to q\bar{q}$: photon wave function Ψ (QED)
2. $q\bar{q}$-target interaction: dipole amplitude N_Ω
3. $q\bar{q} \to \mathrm{J}/\psi$: J/ψ wave function $\Psi_{\mathrm{J}/\psi}$

Dipole: MV model + JIMWLK evolution constrained by HERA data (backup)

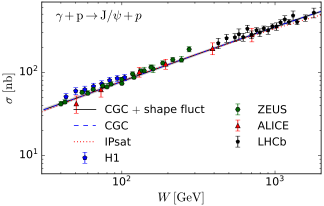

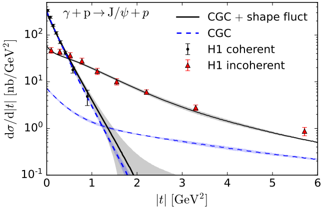

H.M, Salazar, Schenke, 2207.03712

No net color charge transfer ("diffractive"), Ω=target configuration

Initial condition

Dipole: MV model + JIMWLK evolution constrained by HERA data

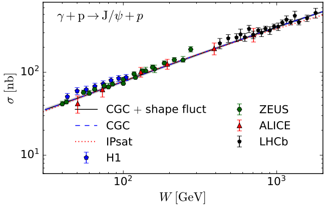

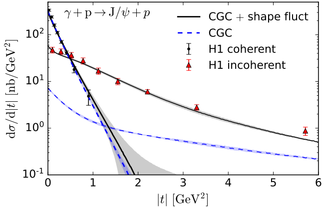

$x = 0.01 \to$ JIMWLK

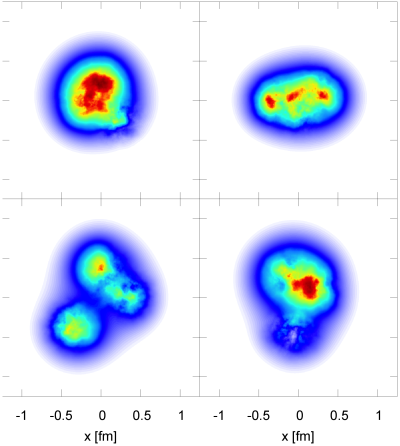

Large e-b-e fluctuations in proton geometry.

H.M, Schenke, 1603.04349 + subsequent papers

Saturation in coherent production: $\gamma + \mathrm{Pb} \to \mathrm{J}/\psi + \mathrm{Pb}$

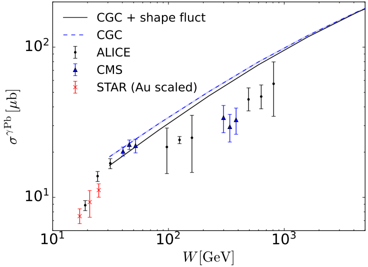

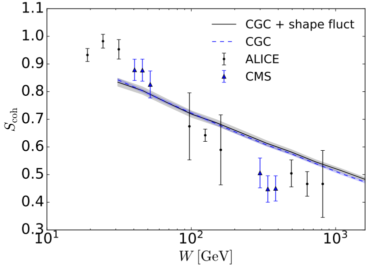

- Challenging to describe the W dependence of $\sigma^{\gamma \mathrm{Pb}}$
  - LHC data well reproduced at moderate $W \lesssim 100$ GeV
  - Energy dependence well reproduced at higher W, but overestimate overall cross section
- Nuclear suppression factor

$$S_{\mathrm{coh}} = \sqrt{\frac{\sigma^{\gamma \mathrm{Pb}}}{\sigma_{\mathrm{IA}}}}, \quad \sigma_{\mathrm{IA}} = \frac{\mathrm{d}\sigma^{\gamma p}}{\mathrm{d}t}\bigg|_{t=0} \int \mathrm{d}t\, |F(t)|^2$$

  - General trend captured...
  - ...but data would prefer a stronger W dependence

No free parameters when moving $p \to A$: genuine prediction

Ongoing work: include $\gamma + \mathrm{Pb}$ to fits determining JIMWLK IC

H.M, Salazar, Schenke, 2312.04194; H.M, Salazar, Schenke, Shen, Zhao, in progress

Saturation in incoherent production: $\gamma + \mathrm{Pb} \to \mathrm{J}/\psi + \mathrm{Pb}^*$

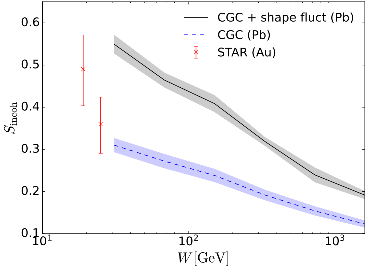

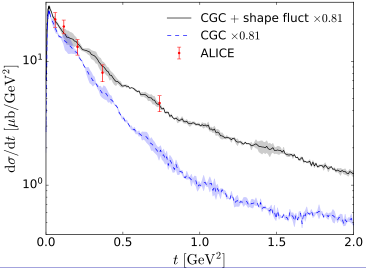

- Proton e-b-e fluctuating geometry tuned to HERA data
- Smoother proton at small-x $\Rightarrow$ reduced fluctuations, incoherent cross section suppressed
- Lower-energy measurement from STAR for the suppression factor

$$S_{\mathrm{incoh}} = \frac{\sigma^{\gamma+\mathrm{Pb}\to\mathrm{J}/\psi+\mathrm{Pb}^*}}{A(\sigma^{\gamma+p\to\mathrm{J}/\psi+p} + \sigma^{\gamma+p\to\mathrm{J}/\psi+p^*})}$$

- LHC data can probe $x_{\mathbb{P}}$ dependent geometry fluctuations
- ALICE t spectra: compatible with no modification to nucleon substructure in nuclei at $x_{\mathbb{P}} \sim 10^{-3}$

H.M, Salazar, Schenke, 2312.04194

Interference patterns (see previous talk for a proper introduction)

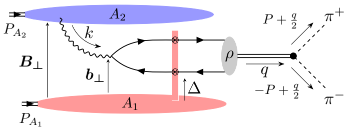

- γ linearly polarized $\uparrow\uparrow \mathbf{B}_\perp$, polarization transferred to ρ
- Effect on decay products, but not visible as $\mathbf{B}_\perp$ random
- But two different amplitudes & interference:

Correlations in daughters $\rho \to \pi^+ + \pi^-$ (or $\mathrm{J}/\psi \to e^+ + e^-$)

$$\frac{\mathrm{d}\sigma^{\rho\to\pi^+\pi^-}}{\mathrm{d}^2\mathbf{P}_\perp \mathrm{d}^2\mathbf{q}_\perp \mathrm{d}y_1 \mathrm{d}y_2} = \text{coherent} + \text{incoherent} =$$

$$\frac{1}{2(2\pi)^3}\frac{f^2}{(M_{\pi\pi}^2 - M_V^2)^2 + M_V^2\Gamma^2}\left\{ \left\langle \int \mathrm{d}^2\mathbf{B}_\perp \mathcal{M}^i(\mathbf{q}_\perp,\mathbf{B}_\perp)\mathcal{M}^{\dagger,j}(\mathbf{q}_\perp,\mathbf{B}_\perp)\mathbf{P}_\perp^i\mathbf{P}_\perp^j\Theta(|\mathbf{B}_\perp| - \underbrace{B_{\min}}_{\text{determine e-b-e}}) \right\rangle_\Omega \right.$$

$$\mathcal{M}^i(y_1,y_2,\mathbf{q}_\perp,\mathbf{B}_\perp) = \int \mathrm{d}^2\mathbf{b}_\perp e^{-i\mathbf{q}_\perp\cdot\mathbf{b}_\perp}\left[\underbrace{\widetilde{\mathcal{A}}_1(x_1,\mathbf{b}_\perp)}_{\gamma+A_1\ \text{scattering}}\ \underbrace{\widetilde{\mathcal{F}}_2^i(x_2,\mathbf{b}_\perp-\mathbf{B}_\perp)}_{\gamma\ \text{field of}\ A_2} + \widetilde{\mathcal{A}}_2(x_2,\mathbf{b}_\perp-\mathbf{B}_\perp)\widetilde{\mathcal{F}}_1^i(x_1,\mathbf{b}_\perp)\right]$$

H.M, Salazar, Schenke, Shen, Zhao, 2310.15300

Interference patterns: $A + A \to A^{(*)} + A^{(*)} + \rho$

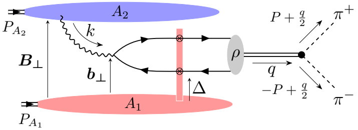

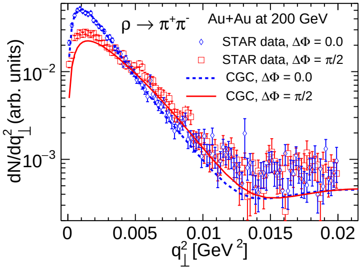

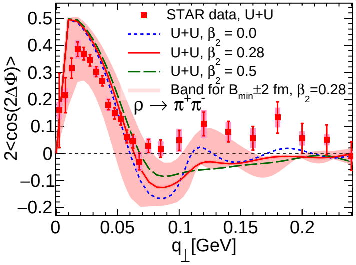

Φ: angle between $\mathbf{P}_\perp + \frac{\mathbf{q}_\perp}{2}$ and $\mathbf{q}_\perp$

- Spectra well described including linearly polarized photons, interference and photon k_T
- Angular modulation sensitive to deformations
  - Dominant reason: different $B_{\min}$ distributions

Caveat: ρ mass not large enough to fully justify perturbative calculation, but modulation insensitive to $r \gtrsim 1$ fm dipoles at $|\mathbf{q}_\perp| < 0.1$ GeV

H.M, Salazar, Schenke, Shen, Zhao, 2310.15300

Interference in different neutron classes: $\mathrm{Pb} + \mathrm{Pb} \to \mathrm{Pb}^{(*)} + \mathrm{Pb}^{(*)} + \rho$

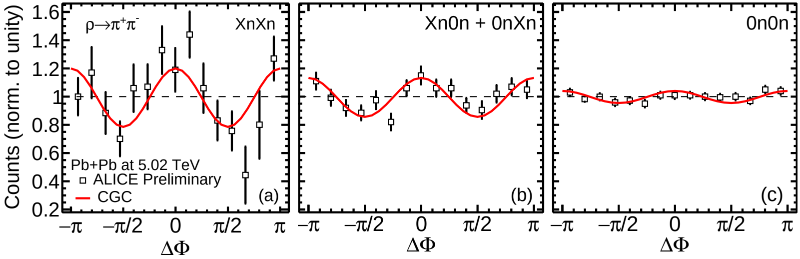

- More neutrons emitted when impact parameter is smaller
- Interference decreases with increasing impact parmeter

H.M, Salazar, Schenke, Shen, Zhao, 2310.15300

Polarized deuteron

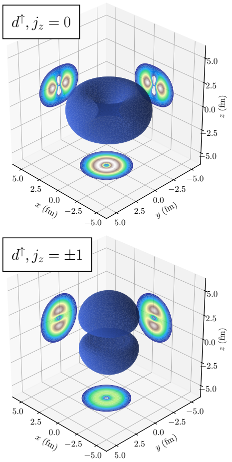

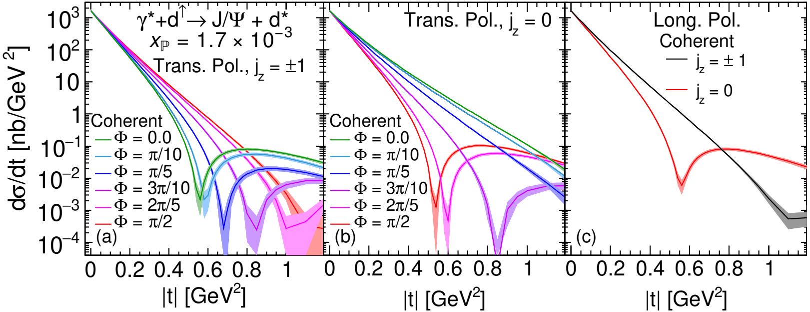

- Unique at the EIC: polarized beams
  $\Rightarrow$ probe spatial distribution of small-x gluons in a polarized d
- Φ: Angle between J/ψ momentum and d polarization
- Effective deuteron size seen depends on the angle

H.M, Salazar, Schenke, Shen, Zhao, in preparation

Conclusions

- $\gamma + \mathrm{Pb}$ data from UPCs: probe saturation in the TeV range
- Strong suppression from the LHC qualitatively understood, but challenging to get as large suppression at high W
  - Note: no free parameters when moving $p \to \mathrm{Pb}$
- Future measurements for incoherent $\gamma + \mathrm{Pb} \to \mathrm{J}/\Psi + \mathrm{Pb}^*$ allow for probing nucleon geometry fluctuations in nuclear environment
- Azimuthal correlations in UPCs sensitive also to deformed structure of nuclei
- EIC possibility: how are small-x gluons distributed in a polarized deuteron?

The 2nd workshop on the physics of Ultra Peripheral Collisions

Ultra Peripheral location for UPC physics

- Lapland, Finland, 9.-13.6.2025 (24h daylight!), TBC
- https://indico.cern.ch/event/1378275/

Local organizing committee chairs

- Ilkka Helenius and Heikki Mäntysaari

Travel

- International flight to Helsinki + domestic connection

Backups

Saturation effect on nuclear geometry: $A+A\to A+A+J/\psi$

$\gamma+\mathrm{Pb}$ at the LHC: very high density, saturation can modify the nuclear geometry

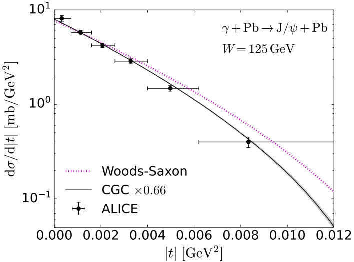

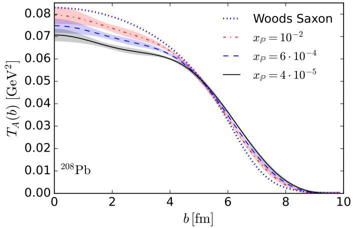

UPC data from LHC: $x=6\cdot10^{-4}$

- Coherent $\gamma+\mathrm{Pb}\to J/\psi+\mathrm{Pb}$
- No saturation: geometry = Woods-Saxon
  $\Rightarrow$ not compatible with ALICE data
- Saturation: nucleus $\approx$ black disc at the center
  $\Rightarrow$ modifieds nuclear geometry
  $\Rightarrow$ J/ψ spectra compatible with ALICE measurements

H.M, Schenke, Salazar, PRD106 (2022), ALICE: PLB817 (2021)

Example with protons: proton shape from $\gamma + p \to J/\Psi + p$

Comparison to HERA data including color charge fluctuations ($x \sim 10^{-3}$)

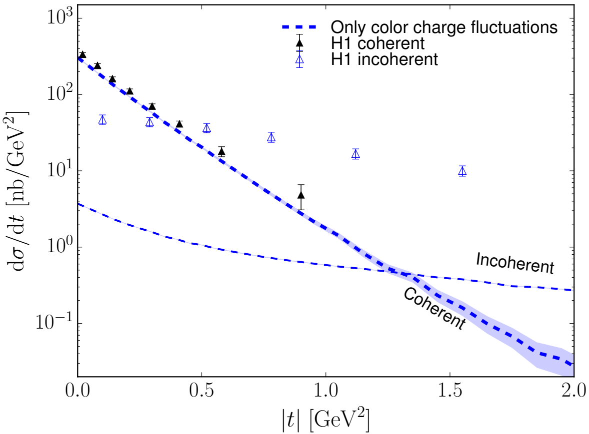

H.M, B. Schenke, PRL 117, 052301 (2016), PRD 94, 034042, H1: EPJC73, 2466

Round proton:

Fit proton size: (gluonic) radius $r_p \sim 0.6$ fm

Note EM radius 0.88 fm

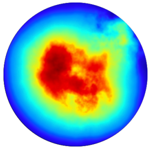

Average geometry (coherent) ✓

Fluctuations (incoherent) ✗

Constraining proton fluctuations: $\gamma + p \to J/\Psi + p$

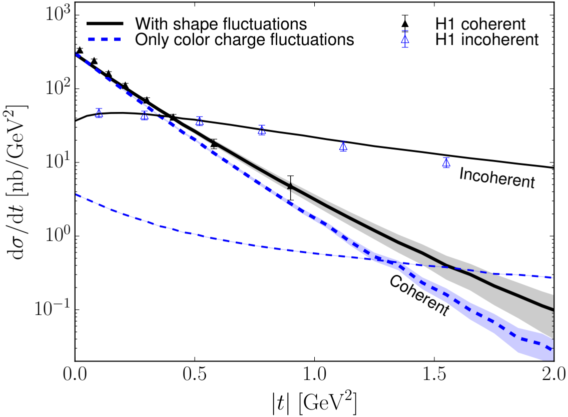

Parametrize e-b-e fluctuating geometry, fit data

Fluctuations

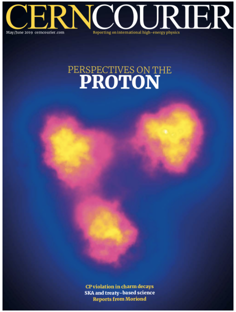

Round

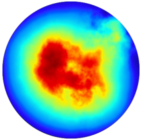

HERA data can be described with large event-by-event fluctuations in the proton geometry

H.M, B. Schenke, PRL 117, 052301 (2016), PRD 94, 034042, H1: EPJC73, 2466

Dipole amplitude from the CGC

Color charge distribution at $x = 0.01$

- Event-by-event random color charge distribution ρ^a
- McLerran-Venugopalan model $g^2\langle\rho^a(\mathbf{x}_\perp)\rho^b(\mathbf{y}_\perp)\rangle \sim \delta^{ab}\delta(\mathbf{x}_\perp - \mathbf{y}_\perp)g^4\mu^2$
- $g^4\mu^2 \sim Q_s^2(\mathbf{b}_\perp) \sim T_p(\mathbf{b}_\perp)$ from IPsat fit to HERA σ_r data

Small-x evolution

- Perturbative JIMWLK evolution (event-by-event)
- Infrared regulator to suppress gluon emission at long distance

Dipole-target amplitude

- $N(\mathbf{r}_\perp = \mathbf{x}_\perp - \mathbf{y}_\perp) = 1 - \frac{1}{N_\mathrm{c}}\langle V^\dagger(\mathbf{x}_\perp)V(\mathbf{y}_\perp)\rangle$
- $V(\mathbf{x}_\perp) = P\exp\left(-ig\int \mathrm{d}x^- \frac{\rho(\mathbf{x}_\perp)}{\nabla^2 - m^2}\right)$

STAR suppression factor data

H.M, Salazar, Schenke, 2312.04194:

Channel	STAR	CGC + shape fluct	CGC
S_{coh}	0.846 ± 0.063	0.89	0.90
S_{incoh}	$0.36^{+0.06}_{-0.07}$	0.58	0.32

Table: Nuclear modification factors for J/ψ photoproduction in $\gamma + \mathrm{Au}$ collisions. The CGC predictions are calculated at $x_{\mathbb{P}} = 0.01$ and the STAR measurements are performed at $x_{\mathbb{P}} = 0.015$. The coherent suppression factors S_{coh} obtained with and without nucleon substructure fluctuations are compatible with each other within the numerical accuracy.